ACS OMEGA

http://pubs.acs.org/journal/acsodf

Article

Modified Thymosin Alpha 1 Distributes and Inhibits the Growth of Lung Cancer in Vivo

Renhao Peng, Caoying Xu, Heng Zheng,* and Xingzhen Lao*

Cite This: *ACS Omega* 2020, 5, 10374−10381

Read Online

ACCESS | Metrics & More | Article Recommendations

ABSTRACT: Targeted therapy of tumors is an effective method for treating cancer. Thymosin alpha 1 (Tα1), a hormone that contains 28 amino acids, is already approved for cancer treatment. However, its clinical application is limited because of the lack of tumor targeting. Considering that RGD can specifically bind to integrin, the anticancer drug can have a targeted therapeutic effect on tumors when it combines with a peptide containing an RGD sequence. We produced a polypeptide, Tα1-RGDR, by binding Tα1 to RGDR. The RGDR can combine with the $\alpha v\beta 3$ and NRP-1 domains, which are highly expressed on the surface of the tumor, to achieve the effect of tumor targeting. This work aimed to investigate the difference of antitumor activity and tumor targeting between Tα1 modified by RGDR and Tα1 by using H460 and LLC tumor models. Results showed that Tα1-RGDR had remarkable antitumor effects, and its tumor targeting was better than that of Tα1. Hence, Tα1-RGDR is a promising antitumor drug.

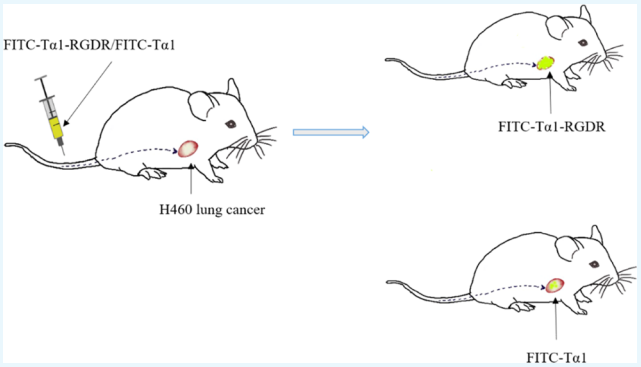

INTRODUCTION

With the development of society, an increasing number of factors, such as cancer, threaten people's health. Lung cancer is one of the leading causes of cancer deaths.[1] In recent years, proteins and peptides have attracted wide attention due to their good efficacy in treating traditional diseases such as cancer.[2] Thymosin alpha1 (Tα1) is one of many polypeptide drugs.[3]

Thymosin alpha 1 (Tα1) is a 28-amino-acid peptide expressed in the thymus.[3] It was originally used as an immune booster and has been used in the treatment of immunodeficiency diseases. As an immunomodulatory compound, Tα1 can significantly upregulate the production of CD4 + T and CD8 + T cells.[4,5] The interaction between immunologically functional cells and immune factors CD4 +/CD8 + T cells can mediate the tumor survival environment and inhibit the growth of gastric cancer cells.[6] In hepatocellular carcinoma, CD4 + T cells mediate cytotoxicity and exert antitumor immunity.[7] Ma et al. also demonstrated that CD4 + T lymphocytes can produce high levels of reactive oxygen species, which can inhibit or delay the development of liver cancer.[8] The role of Tα1 in immunodeficiency mainly includes the promotion of response between dendritic cells and antibodies, down-regulation of thymocyte apoptosis, and upregulation of cytokines and chemokines.[9,10] The maturation of T lymphocytes is derived from the mitosis of peripheral blood lymphocytes stimulated by many factors, including Tα1. Tα1 plays an important role in enhancing immunity in the body's immune organs and tissues. Tα1 not only promotes T lymphocyte maturation and increases lymphocyte levels, such as interferon-γ (IFN-γ) and interleukin-2 (IL-2),[11,12] but also enhances lymphocyte response by activating CD4 cells.[13] With the great progress in cancer immunotherapy, Tα1 has been applied to the clinical treatment of cancer.[14] Tα1 can help to present antigens at the time of tumor production, thus facilitating the induction of immune response and identification of tumor cells.[15] Tα1 has superior medical effects in the treatment of advanced nonsmall cell lung cancer[16,17] and melanoma.[18−20]

However, Tα1 has antitumor activity; when it acts on tumor cells, it also acts on normal cells and causes a series of side effects, thus limiting its clinical use. In previous studies, Tα1-modified peptides or Tα1 in combination with other drugs have shown better antitumor activity than Tα1 alone.[21,22] RGD (Arg-Gly-Asp)[23] and iRGD (CRGDKGPDC)[22] have been utilized in delivering a limited number of anticancer drugs to tumor sites to increase the effects of anticancer drugs. To deliver Tα1 more efficiently to tumor tissues, we designed a

Received: January 16, 2020
Accepted: April 13, 2020
Published: April 27, 2020

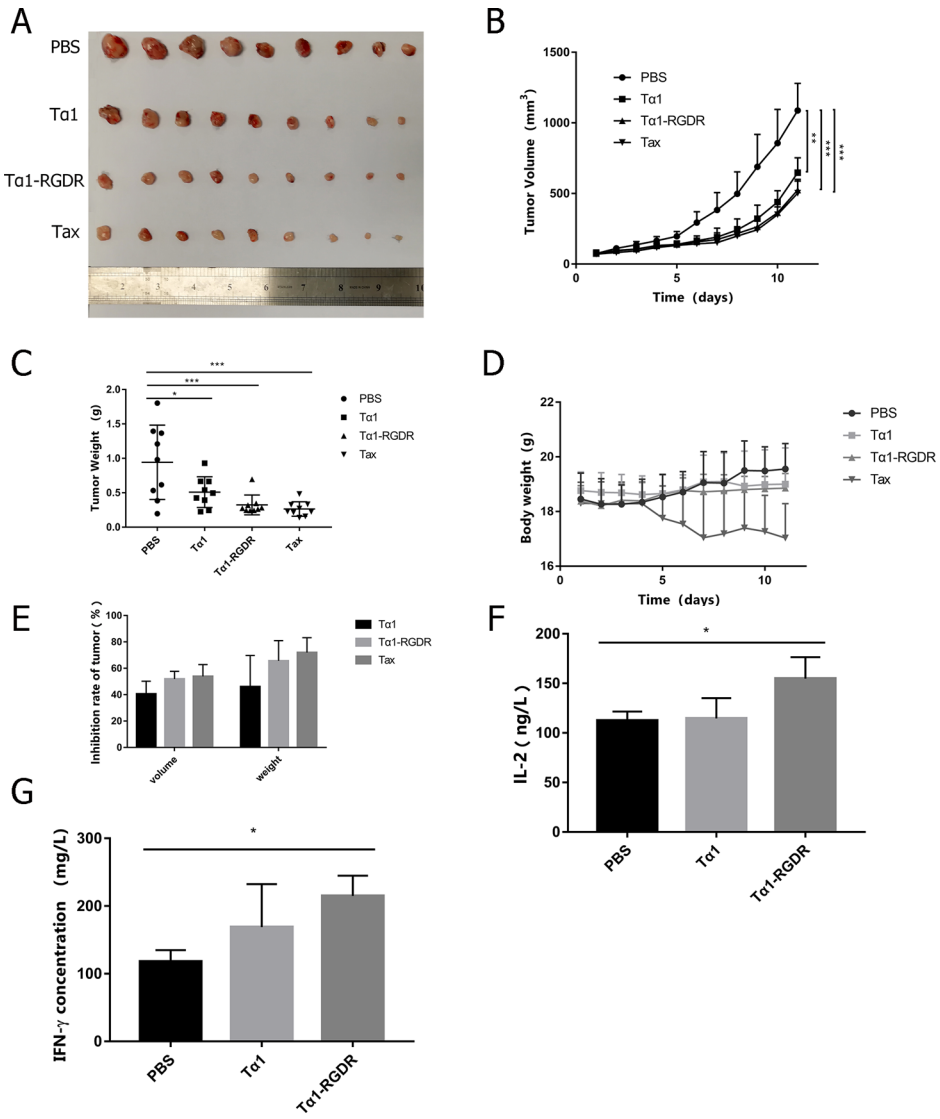

Figure 1. Inhibitory effect of Tα1-RGDR on LLC tumor model. (A) Tumor mass and entity photo of tumors (n = 9). (B) Tumor volume changes in different treatment groups (n = 9). LLC cells were injected subcutaneously into the left forelimb of C57BL/6 mice (5×10^5 cells/mouse). The tumor volume grew to 80−100 mm^3, and the mice were randomly divided into four groups. Then, 0.1 mL of PBS, 0.31 mg/kg of Tα1-RGDR, and 0.25 mg/kg Tα1 were continuously injected subcutaneously every day, whereas 10 mg/kg of paclitaxel (Tax) was injected every other day. The mice were sacrificed, and the tumors were separated after the tumor volumes in the negative group reached approximately 1000 mm^3. (C) Tumor weight in different groups (n = 9). (D) Mouse weight changes in different groups (n = 9). (E) Antitumor inhibition ratio of tumor mass and volume. (F) Histogram of IL-2 levels in mouse serum (n = 4). (G) Histogram of IFN-γ levels in mouse serum (n = 4). *$p < 0.05$, **$p < 0.01$, ***$p < 0.001$.

new peptide, Tα1-RGDR.[24] RGDR contains an RGD sequence that can bind to integrin $\alpha v\beta 3$, which is overexpressed in many tumor surfaces. Tα1-RGDR also contains an RGDR sequence, which has a C-terminal R/KXXR/K motif that can bind with Neuropilin-1 (NRP-1), a cellular receptor expressed on the surface of tumors and involved in the regulation of tumor vascular permeability.[24−26] Integrins and neuropilin are major factors in tumor-targeting peptides.[27] Integrin is one of the main family members of cell surface receptors, and it mediates the adhesion of cell and extracellular matrix.[28] $\alpha v\beta 3$, a highly expressed integrin, is involved in tumor angiogenesis, invasion, and metastasis.[29] Given the high expression of $\alpha v\beta 3$ on tumor surfaces and in endothelial cells during neovascularization, integrin $\alpha v\beta 3$ has been the target of many antitumor angiogenic drugs.

Hence, we bound RGDR to the C-term of Tα1 by using a GGGG linker to form a polypeptide, Tα1-RGDR.[24] Ta1-RGDR not only effectively inhibits tumor growth in a mouse melanoma tumor model but also greatly enhances mouse immunodeficiency disease induced by hydrocortisone.[24] In this study, we aimed to explore the antitumor activity and tumor-targeting ability of Tα1-RGDR for lung cancer.

RESULTS

Tα1-RGDR Inhibited LLC Tumor Growth in Mice in Vivo. The tumor volume and body weight of mice in each group were measured daily, and their growth status was observed. After the administration, tumor-bearing mice were euthanized to obtain tumors, as shown in Figure 1A. No significant difference in tumor volume was observed between groups during the first 3 days of administration. After 4 days of

https://dx.doi.org/10.1021/acsomega.0c00220
ACS Omega 2020, 5, 10374−10381

administration, the tumor volume increased significantly in the PBS group but slowly in the Tα1-RGDR group, with tumor volume approaching that of the Tax group (Figure 1B). Figure 1A shows that the median tumor mass in the PBS group was significantly larger than that in the Tax and Tα1-RGDR groups, and the difference in tumor weight between the Tα1-RGDR and PBS groups was less than 0.001 (p = 0.0008) (Figure 1C). The tumor weight of the Tα1-RGDR group was lower than that of the Tα1 group, indicating its advantage in inhibiting the growth of LLC tumor. After 4 days of Tax treatment on C57BL/6 mice bearing LLC tumors, the body weight of the mice decreased sharply, the mice were in a state of mental dystrophy, and food intake was reduced. The mice in the Tα1-RGDR group showed no similar symptoms (Figure 1D). In the LLC tumor model group, after 11 days of administration, the average tumor volumes in the PBS group, Tα1 group, and Tα1-RGDR and Tax groups reached 1100, 650, and 520 and 500 mm^3, respectively. After the administration, the tumor volume inhibition rate induced by Tα1-RGDR was 51.83 ± 5.8% compared with that of the PBS group, whereas the tumor volume inhibition rate in the Tα1 group was only 40.5 ± 9.7%. The difference in the tumor volume inhibition rate between the PBS and Tα1-RGDR groups was more significant than that of the PBS and Tα1 groups (Figure 1E). Mice carrying tumors derived from LLC cells were treated with Tα1-RGDR for 11 days. Blood was then taken from the peripheral area, and IFN-γ or IL-2 cytokine was measured by ELISA. The levels of IL-2 and IFN-γ in the Tα1-RGDR group were 154.78 ± 21.70 and 214.76 ± 30.20 ng/L, respectively, whereas those in the Tα1 treatment group were only 114.62 ± 25.50 and 168.99 ± 30.20 ng/L. Compared with the Tα1 group, mice bearing LLC after Tα1-RGDR treatment had significantly increased levels of IL-2 and IFN-γ (Figure 1F,G).

Pathological Tissue Section from LLC Tumor Models. After 11 days of administration, tumor-carrying mice were dissected to obtain tumors. Histochemistry and immunohistochemistry (IHC) results showed that the Tα1-RGDR group could promote the infiltration of CD4 and CD8 into tumor tissues. H&E staining of tumor tissues showed severe necrosis of tumor tissues in the Tα1 and Tα1-RGDR groups, and the necrosis area was large (Figure 2). Compared with those in the Tα1 group, CD4 + T and CD8 + T in the Tα1-RGDR group greatly infiltrated into tumor tissues. The IHC of CD31 showed that both Tα1 and Tα1-RGDR reduced the amount of CD31, but the reduction was not significant in the Tα1 group (Figure 3).

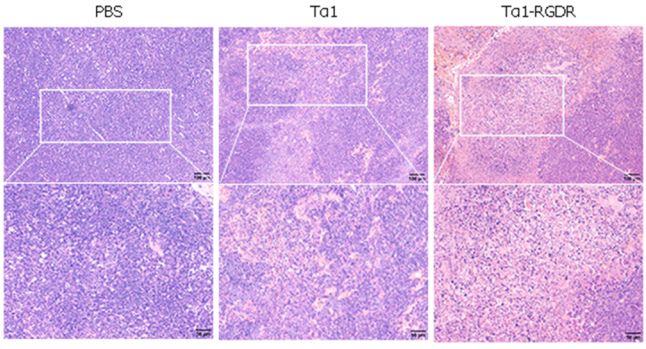

Figure 2. HE staining of LLC tumor sections.

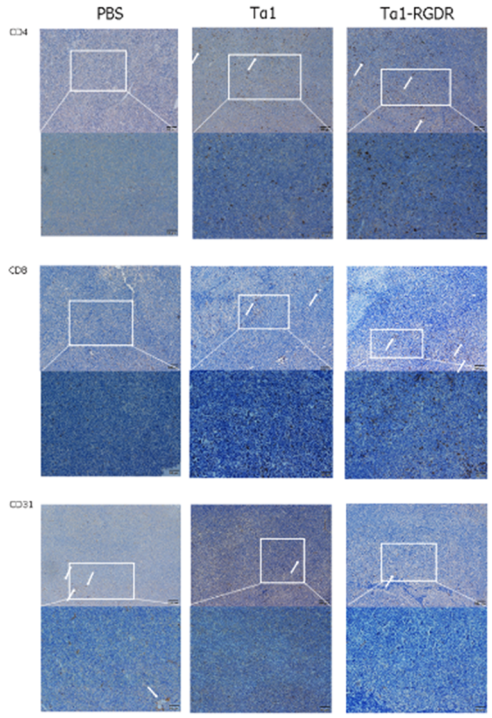

Figure 3. Expression patterns of CD4, CD8, and CD31 in LLC tumor sections. Immunohistochemical staining of CD4, CD8, and CD31 in lung cancer tissues. Expression of CD4, CD8, and CD31 in LLC tumor xenograft tissues following treatment with PBS, Tα1, and Tα1-RGDR. White arrows represent the positive cytoplasm of CD4, CD8, and CD31 staining (200× magnification). Brown staining indicates positive CD4, CD8, and CD31 expression, whereas blue staining indicates cell nuclei.

Therefore, Tα1-RGDR had better effects in promoting the infiltration of CD4 and CD8 into tumor tissues and downregulating CD31 compared with Tα1.

Tα1-RGDR Interfered with H460 Growth in Vivo. Equimolar amount of Tα1 and Tα1-RGDR (0.081532 μmol/kg) was administrated in the experiment. Extracted tumors from BALB/c mice were lined as shown in Figure 4A. The tumor volume of every seven mice in each group was measured every day for 11 consecutive days. As time went by, tumors grew more quickly. The average tumor volume of the PBS group on day 11 reached 904.89 ± 298.99 mm^3, whereas those of Tα1, Tα1-RGDR, and Tax were 198.47, 339.19 ($p < 0.05$), and 501.91 mm^3 ($p < 0.01$) lower than that of the PBS group, respectively (Figure 4B). On the basis of the tumor weight scatter spot, the tumor size was more ordered and had a lower SD value in the Tα1-RGDR group (Figure 4C). After 11 days of administration, the tumors were dissected and weighed, and a significant difference was observed in the tumor weight between PBS and Tα1-RGDR (Figure 4C, p = 0.018). The tumor weight in the Tα1-RGDR group was lower than that in the Tα1 group, and the tumor weight difference in the Tax group was verified, showing superior homogeneity. Therefore, Tα1-RGDR could better inhibit tumor growth than Tα1.

Except for the Tax administration group, no group showed obvious abnormal effects, such as loss of body weight (Figure 4D). The tumor inhibition rate with the average tumor volume or tumor weight of PBS group as a benchmark was calculated and is shown in Figure 3E. The tumor inhibition rates of Tα1-RGDR on tumor volume and weight were 37.48 and 46.62%,

https://dx.doi.org/10.1021/acsomega.0c00220
ACS Omega 2020, 5, 10374−10381

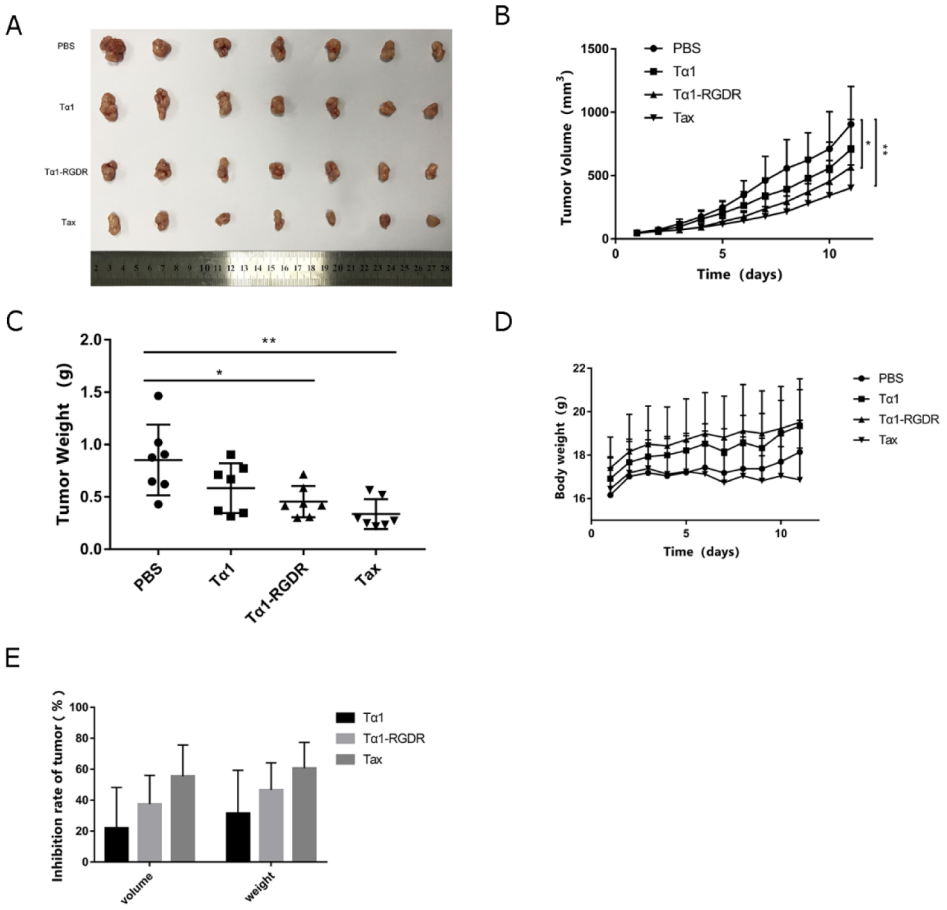

Figure 4. Inhibitory effect of Tα1-RGDR on H460 tumor model. (A) Tumor mass and entity photo of tumors (n = 7). (B) Tumor volume changes in different treatment groups (n = 7). H460 cells were injected subcutaneously into the left forelimb of BALB/c nude mice (5×10^5 cells/mouse). The tumor volume grew to 80−100 mm^3, and the mice were randomly divided into four groups. Then, 0.1 mL of PBS, 0.31 mg/kg of Tα1-RGDR, and 0.25 mg/kg of Tα1 were continuously injected subcutaneously every day, whereas 10 mg/kg of paclitaxel (Tax) was injected every other day. The mice were sacrificed, and the tumors were separated after the tumor volumes in the negative group reached approximately 1000 mm^3. (C) Tumor weight in different groups (n = 7). (D) Mouse weight changes in different groups (n = 7). (E) Antitumor inhibition ratio of tumor mass and volume.

whereas those of Tα1 were 21.9 and 31.5%, respectively. In sum, Tα1-RGDR can inhibit H460 tumor progression compared with Tα1 without causing obvious side effects.

Pathological Tissue Section from H460 Tumor Models. In pathological HE slices, the nucleus was stained purple, whereas the cytoplasm was stained pink. A considerable quantity of cells stained as purple from the PBS group tumor was close to each other, whereas the pink area occupied a small part of the whole slice. After Tα1 administration, more pink areas were observed and had much lower quantity of cells, which have been shrunk. In Tα1-RGDR group slices, these effects were more robust: the pink area increased, indicating intensive necrosis (Figure 5A).

CD31 antibody was used to locate the growth of vasculature in tumor. As shown in Figure 4, cells that did not express CD31 were stained blue, whereas cells that expressed CD31 were brown. Brown strips were observed in the PBS group slices. Tα1 and Tα1-RGDR reduced the amount of CD31. Strips in Tα1 group were much shorter than those in the PBS group; however, the quantity was reduced insignificantly. Compared with Tα1, Tα1-RGDR reduced CD31 expression (Figure 5B). Hence, Tα1-RGDR showed a stronger activity in promoting tumor necrosis and downregulating vasculature than Tα1.

Specific Targeting of Tα1-RGDR in Vivo. BALB/c nude mice bearing H460 tumor were chosen to investigate the in vivo distribution of FITC-labeled Tα1-RGDR. After 2 h of internalization in the mice system, important entities were visualized, as shown in Figure 6. Tumors from the Tα1-RGDR group and Tα1 group were in the same scale of tumor size. The fluorescence intensity of the Tα1-RGDR group was 2.929e + 08, while the fluorescence intensity of the Tα1 group was only 1.626e + 08. The fluorescence intensity of the Tα1-RGDR group was 1.8 times that of the Tα1 group, and the fluorescence covered more than 90% of the tumor area. At the same time, fluorescence intensity was detected in the lungs of the Tα1-RGDR group mice, and H460 was detected as a tumor cell derived from human lungs in the fluorescence intensity of the Tα1 group. In addition, the fluorescence intensity of the liver in the Tα1-RGDR group was stronger. These findings indicate that in the H460 lung cancer model, more Tα1-RGDR is targeted to tumor than Tα1.

DISCUSSION

Our laboratory used RGDR bound to the C-terminus of Tα1 with GGGG linker between them to form a novel polypeptide, Tα1-RGDR.[24] We found that the tumor volume and tumor weight were much smaller in the mice treated with Tα1-RGDR

https://dx.doi.org/10.1021/acsomega.0c00220
ACS Omega 2020, 5, 10374−10381

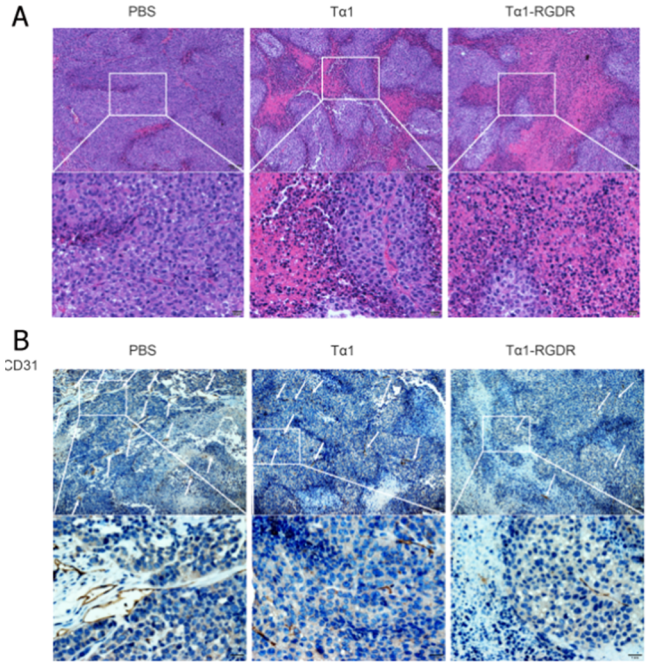

Figure 5. HE and IHC in H460 tumor sections. (A) HE staining of H460 tumor sections. (B) Immunohistochemical staining of CD4, CD8, and CD31 in lung cancer tissues. Expression of CD4, CD8, and CD31 in H460 tumor xenograft tissues following treatment with PBS, Tα1, and Tα1-RGDR. White arrows represent the positive cytoplasm of CD4, CD8, and CD31 staining (200× magnification). Brown staining indicates positive CD4, CD8, and CD31 expression, whereas blue staining indicates cell nuclei.

than with Tα1 in LLC and H460 tumor models. Tα1 was originally used as an immunomodulator for the treatment of chronic hepatitis B.[30−32] Tα1 can enhance the immune response of T cells by increasing the number of CD4 + T cells and promoting the release of IL-2 and INF-γ.[33,34] Now, Tα1 has been applied for the treatment of tumors. The interaction between immunologically functional cells and immune factors CD4 +/CD8 + T cells can mediate the tumor survival environment and inhibit the growth of gastric cancer cells.[6] In hepatocellular carcinoma, CD4 + T cells mediate cytotoxicity and exert antitumor immunity.[7] Ma et al. also demonstrated that CD4 + T lymphocytes can produce high levels of reactive oxygen species, which can inhibit or delay the development of liver cancer.[8] Tα1 can significantly upregulate the production of CD4 + T and CD8 + T cells,[4,5] and the same results were observed in our experiments. After the LLC-bearing mice were treated with the Tα1-RGDR peptide, CD4 + T and CD8 + T cells infiltrated into cancer cells, and the expression levels of cytokines such as IFN-γ and IL-2 increased. IFN-γ and IL-2 can promote the activation of immune cells, and IFN-γ can induce tumor regression.[35,36] Inhibiting tumor angiogenesis is an effective treatment for cancer.[37] CD31 is a member of the immune protein superfamily expressed in T cells and B cells,[38] and CD31 is also expressed in many tumor cells.[39,40] Today, CD31 is used to demonstrate the presence of endothelial tissue and assess tumor angiogenesis and tumor cell invasion.[39,41] Pathological tissue section from H460 tumor models showed that Tα1-RGDR reduced CD31 expression. These results explain why Tα1-RGDR is a more promising antitumor drug than Tα1.

When used in combination with other drugs, Tα1 shows significant therapeutic potential in tumor treatment.[18,19] However, the lack of tumor targeting has limited the application of Tα1 in the clinical treatment of tumors. In order to exert the antitumor function of Tα1, our laboratory has designed a new tumor-targeting peptide, Tα1-RGDR. Our experimental results shown that Tα1-RGDR has better antitumor activity than Tα1, and its effect in inhibiting tumor growth is close to that of paclitaxel. Significant results have been obtained with Tα1-RGDR in the H460 tumor model for the treatment of lung cancer. Tα1-RGDR significantly inhibited tumor growth at the same dose as Tα1. In addition, higher levels of tumor-specific targeting and less angiogenesis were observed in H460 tumor-bearing mice treated with Tα1-RGDR. In in vivo fluorescence experiments, Tα1-RGDR was more targeted to tumor tissue than Tα1. The results of this experiment demonstrated that RGDR is a key factor that causes Tα1 to target tumors. Recent studies have provided clues as to how RGDR-modified Tα1 mediates tumor homing. The RGDR sequence contains the RGD sequence, which can bind to integrin $\alpha v\beta 3$ that is overexpressed in many tumors. Peptides containing RGD can induce tumor cell death and significantly inhibit tumor growth.[42] NRP-1, a transmembrane glycoprotein, is widely expressed in tumor tissues

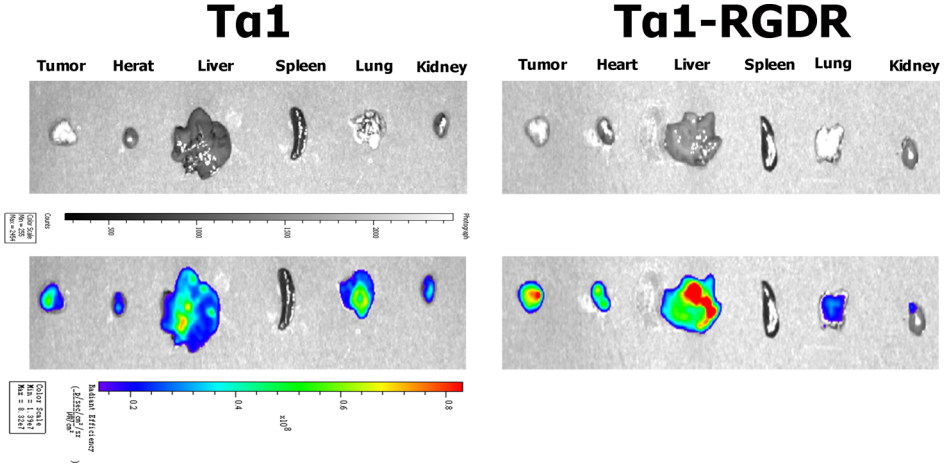

Figure 6. Specific targeting of Tα1-RGDR in vivo. BALB/c nude mice bearing H460 tumor cells were chosen to investigate the in vivo distribution of FITC-labeled Tα1-RGDR. The closer the color of fluorescence is to red, the stronger the fluorescence.

https://dx.doi.org/10.1021/acsomega.0c00220
ACS Omega 2020, 5, 10374−10381

and plays a crucial role in tumor angiogenesis.[43] Integrin $\alpha v\beta 3$, an integrin protein closely associated with tumor angiogenesis, specifically recognizes the RGD sequence.[44] Peptides containing the RGD sequence interact with integrins by proteolysis to generate a C-terminal consensus sequence which then binds to highly expressed NRP-1 on tumor cells, thereby targeting tumor cells.[45] Such as cilengitide [c(-RGDf(NMe)V-)].[46] These pieces of evidence indicate that RGDR is the main factor leading to the tumor-targeting effect of Tα1. These experimental results demonstrated the effectiveness of Tα1-RGDR in the treatment of nonsmall cell lung cancer and also provided new options for cancer treatment.

CONCLUSIONS

LLC and H460 tumor models have proven that Tα1-RGDR not only has similar antitumor effects to paclitaxel in the treatment of lung cancer but also does not have the adverse conditions of weight loss and mental depression in mice after administration of paclitaxel. At the same time, Tα1-RGDR is far superior to Tα1 in reducing systemic toxicity in mice. These results reveal a promising future for Tα1-RGDR in cancer treatment.

EXPERIMENTAL PROCEDURES

Materials. The human lung cancer cell line H460 and mouse lung cancer cell line LLC were purchased from the Cell Bank of the Chinese Academy of Sciences (Shanghai, China). Paclitaxel (Tax) was provided by Yifu Hospital of Nanjing Medical University (Nanjing, Jiangsu Province, China). C57BL/6 mice and BALB/c nude mice were purchased from the Comparative Medicine Center of Yangzhou University (Yangzhou, Jiangsu Province, China). Tα1-RGDR and Tα1 and their FITC-labeled peptides were synthesized by Apeptide Co., Ltd. (Shanghai, China). Mouse-IFN-γ and mouse-IL-2 enzyme-linked immunosorbent assay (ELISA) kits were purchased from Wuhan Boster Bio-Engineering Co., Ltd. (Wuhan, China). Anti-CD4, anti-CD8, and anti-CD31 were purchased from Abcam Ltd. (Nanjing, Jiangsu Province, China).

LLC Tumor Cell Implantation and C57BL/6 Mouse Treatment. All animal experiments complied with the rules and regulations of Contract 2016(su)-0010 with the approval of Jiangsu Provincial Experimental Animal Management Committee. LLC tumor cells were cultured in DMEM containing 10% V/V fetal bovine serum (FBS) and 1% V/V penicillin and streptomycin. LLC tumor cells ($\sim 5 \times 10^5$ cells/mouse) were subcutaneously injected into the left forelimb of C57BL/6 mice. When the tumor volume reached approximately 80 mm^3, the mice were randomly divided into four groups (nine mice/group): PBS, Tα1, Tα1-RGDR, and Tax. Tumor volume was calculated as follows: tumor volume = 0.5 $\times$ (length $\times$ width^2). Then, the mice were administered subcutaneously daily with Tax (10 mg/kg); PBS once daily; and Tα1 and Tα1-RGDR at doses of 0.25 and 0.308 mg/kg (equimolar amount), respectively, in 0.1 mL of PBS once daily for 11 days. The length, width of tumors, weight of mice, and any abnormal conditions were measured daily.

Histochemistry and IHC. The mice were euthanized at the end of the experiment. Tumor tissues were collected and fixed with 4% paraformaldehyde for hematoxylin and eosin (H&E) staining. The fixed tumor tissue sections were incubated with 3% H_2O_2 for 10 min at room temperature, followed by incubation with primary antibody (CD4, CD8, and CD31) for 12 h at 37 °C. Finally, an enzyme-labeled secondary antibody (HRP polymer) was added and incubated for 30 min at room temperature and stained with hematoxylin. The tumor sections were placed under a microscope to observe the infiltration of lymphocytes in the tumor.

Determination of Cytokines IFN-γ and IL-2. C57BL/6 mice in the LLC tumor model group were euthanized when the average tumor volume in the PBS group reached approximately 1100 mm^3. Peripheral blood was first obtained and placed at room temperature for 30 min. Blood samples were centrifuged for 10 min at 4000 rpm, and the supernatant was collected, which was then determined using the mouse IFN-γ or IL-2 kit. IFN-γ or IL-2 standard solution was prepared at a series of concentrations. Approximately 50 μL of blood samples was added to 96-well plates coated with anti-IFN-γ or anti-IL-2 antibodies, incubated at 37 °C for 30 min in a shaker, and then discarded. The 96-well plate was washed five times with mouse-IFN-γ or mouse-IL-2 wash solution. Subsequently, enzyme-labeled reagents were added and incubated at room temperature. The sample was washed again for five times by using the wash solution. The chromogenic agent was added to each well and incubated in the dark at 37 °C for 10 min. To stop the reaction, 50 μL of termination fluid (blue immediately turns yellow) was added to each hole. Finally, the blank hole was adjusted to zero, and the absorbance of each hole was measured successively at 450 nm with a microplate reader.

H460 Tumor Cell Implantation and BALB/c Nude Mouse Treatment. H460 tumor cells were cultured in RPMI-1640 medium containing 10% V/V FBS and 1% V/V penicillin and streptomycin. H460 tumor models were established by injecting 100 μL H460 tumor cell suspension into the mid-left side of BALB/c nude mice subcutaneously ($\sim 5 \times 10^5$ cells/mouse). Groups were divided when the average tumor volume reached approximately 80−100 mm^3. Then, the mice were subcutaneously administered with Tax (10 mg/kg) every day; PBS once daily; and Tα1 and Tα1-RGDR at doses of 0.25 and 0.308 mg/kg (equimolar amount), respectively, in 0.1 mL of PBS once daily for 11 days. The length, width of tumors, weight of mice, and any abnormal conditions were measured daily.

In Vivo Distribution of FITC-Labeled Tα1-RGDR and Tα1. After the establishment of BALB/c nude mouse H460 tumor model, 9 mg/kg of FITC-labeled Tα1-RGDR or Tα1 was then injected into the tail vein of mice. After 0.5 h, the mice were swabbed with alcohol to remove excess fluorescence. After 2 h, the mice were euthanized and dissected to obtain the tumor and their vital organs, such as the heart, liver, spleen, lung, and kidney, which were revealed under the IVIS Spectrum in vivo imaging system (PE, American).

Statistical Analysis. All statistical analyses were performed using SPSS 25.0 software. Numerical data were presented as mean ± SEM. Differences among groups were analyzed using one-way analysis of variance. $P < 0.05$ was considered statistically significant ($^*p < 0.05$; $^{**}p < 0.01$; $^{***}p < 0.001$).

AUTHOR INFORMATION

Corresponding Authors

Heng Zheng − *Department of Life Science and Technology, China Pharmaceutical University, 211199 Nanjing, P. R. China*; Email: zhengh18@hotmail.com

https://dx.doi.org/10.1021/acsomega.0c00220
ACS Omega 2020, 5, 10374−10381

Xingzhen Lao − *Department of Life Science and Technology, China Pharmaceutical University, 211199 Nanjing, P. R. China;* orcid.org/0000-0003-0401-0663; Phone: 86-25-86385398; Email: lao@cpu.edu.cn; Fax: 86-25-86385398

Authors

Renhao Peng − *Department of Life Science and Technology, China Pharmaceutical University, 211199 Nanjing, P. R. China*

Caoying Xu − *Department of Life Science and Technology, China Pharmaceutical University, 211199 Nanjing, P. R. China*

Complete contact information is available at: https://pubs.acs.org/10.1021/acsomega.0c00220

Notes

The authors declare no competing financial interest.

■ ACKNOWLEDGMENTS

This work was supported by the National Natural Science Foundation of China (Grant nos. 31300643 and 31370505), a Project Funded by the Priority Academic Program Development of Jiangsu Higher Education Institutions (PAPD) and Top-notch Academic Programs Project of Jiangsu Higher Education Institutions (TAPP). This work was also supported by the Fundamental Research Funds for the Central Universities (Grant no. 2632018ZD04). The funders had no role in study design, data collection and analysis, decision to publish, or preparation of the manuscript.

■ REFERENCES

(1) Brody, H. Lung cancer. *Nature* **2014**, *513*, S1.

(2) Ibraheem, D.; Elaissari, A.; Fessi, H. Administration strategies for proteins and peptides. *Int. J. Pharm.* **2014**, *477*, 578−589.

(3) Goldstein, A. L.; Goldstein, A. L. From lab to bedside: emerging clinical applications of thymosin alpha 1. *Expert Opin. Biol. Ther.* **2009**, *9*, 593−608.

(4) Jia, Z.; Feng, Z.; Tian, R.; Wang, Q.; Wang, L. Thymosin alpha1 plus routine treatment inhibit inflammatory reaction and improve the quality of life in AECOPD patients. *Immunopharmacol. Immunotoxicol.* **2015**, *37*, 388−392.

(5) Baumann, C. A.; Badamchian, M.; Goldstein, A. L. Thymosin alpha1 is a time and dose-dependent antagonist of dexamethasone-induced apoptosis of murine thymocytes in vitro. *Int. J. Immunopharmacol.* **2000**, *22*, 1057−1066.

(6) Li, F.; Sun, Y.; Huang, J.; Xu, W.; Liu, J.; Yuan, Z. CD4/CD8 + T cells, DC subsets, Foxp3, and IDO expression are predictive indictors of gastric cancer prognosis. *Cancer Med.* **2019**, *8*, 7330.

(7) Meng, F.; Zhen, S.; Song, B. HBV-specific CD4+ cytotoxic T cells in hepatocellular carcinoma are less cytolytic toward tumor cells and suppress CD8+ T cell-mediated antitumor immunity. *APMIS* **2017**, *125*, 743−751.

(8) Ma, C.; Kesarwala, A. H.; Eggert, T.; Medina-Echeverz, J.; Kleiner, D. E.; Jin, P.; Stroncek, D. F.; Terabe, M.; Kapoor, V.; ElGindi, M.; Han, M.; Thornton, A. M.; Zhang, H.; Egger, M.; Luo, J.; Felsher, D. W.; McVicar, D. W.; Weber, A.; Heikenwalder, M.; Greten, T. F. NAFLD causes selective CD4(+) T lymphocyte loss and promotes hepatocarcinogenesis. *Nature* **2016**, *531*, 253−257.

(9) Li, J.; Liu, C. H.; Wang, F. S. Thymosin alpha 1: biological activities, applications and genetic engineering production. *Peptides* **2010**, *31*, 2151−2158.

(10) Moretti, S.; Oikonomou, V.; Garaci, E.; Romani, L. Thymosin alpha1: burying secrets in the thymus. *Expert Opin. Biol. Ther.* **2015**, *15*, 51−58.

(11) Shao, C.; Tian, G.; Huang, Y.; Liang, W.; Zheng, H.; Wei, J.; Wei, C.; Yang, C.; Wang, H.; Zeng, W. Thymosin alpha-1-transformed Bifidobacterium promotes T cell proliferation and maturation in mice by oral administration. *Int. Immunopharmacol.* **2013**, *15*, 646−653.

(12) Wolf, G. T.; Hudson, J.; Peterson, K. A.; Poore, J. A.; McClatchey, K. D. Interleukin 2 receptor expression in patients with head and neck squamous carcinoma. Effects of thymosin alpha 1 in vitro. *Arch. Otolaryngol., Head Neck Surg.* **1989**, *115*, 1345−1349.

(13) Shen, X.; Wang, L.; Xu, C.; Yang, J.; Peng, R.; Hu, X.; Wang, F.; Zheng, H.; Lao, X. Fusion of thymosin alpha 1 with mutant IgG1 CH3 prolongs half-life and enhances antitumor effects in vivo. *Int. Immunopharmacol.* **2019**, *74*, 105662.

(14) Costantini, C.; Bellet, M. M.; Pariano, M.; Renga, G.; Stincardini, C.; Goldstein, A. L.; Garaci, E.; Romani, L. A Reappraisal of Thymosin Alpha1 in Cancer Therapy. *Front. Oncol.* **2019**, *9*, 873.

(15) Garaci, E.; Pica, F.; Serafino, A.; Balestrieri, E.; Matteucci, C.; Moroni, G.; Sorrentino, R.; Zonfrillo, M.; Pierimarchi, P.; Sinibaldi-Vallebona, P. Thymosin alpha1 and cancer: action on immune effector and tumor target cells. *Ann. N. Y. Acad. Sci.* **2012**, *1269*, 26−33.

(16) Garaci, E.; Lopez, M.; Bonsignore, G.; Giulia, M. D.; D'Aprile, M.; Favalli, C.; Rasi, G.; Santini, S.; Capomolla, E.; Vici, P.; et al. Sequential chemoimmunotherapy for advanced non-small cell lung cancer using cisplatin, etoposide, thymosin-alpha 1 and interferon-alpha 2a. *Eur. J. Cancer* **1995**, *31*, 2403−2405.

(17) Salvati, F.; Rasi, G.; Portalone, L.; Antilli, A.; Garaci, E. Combined treatment with thymosin-alpha1 and low-dose interferon-alpha after ifosfamide in non-small cell lung cancer: a phase-II controlled trial. *Anticancer Res.* **1996**, *16*, 1001−1004.

(18) Danielli, R.; Fonsatti, E.; Calabrò, L.; Giacomo, A. M. D.; Maio, M. Thymosin alpha1 in melanoma: from the clinical trial setting to the daily practice and beyond. *Ann. N. Y. Acad. Sci.* **2012**, *1270*, 8−12.

(19) Maio, M.; Mackiewicz, A.; Testori, A.; Trefzer, U.; Ferraresi, V.; Jassem, J.; Garbe, C.; Lesimple, T.; Guillot, B.; Gascon, P.; Gilde, K.; Camerini, R.; Cognetti, F.; Thymosin Melanoma Investigation, G. Large randomized study of thymosin alpha 1, interferon alfa, or both in combination with dacarbazine in patients with metastatic melanoma. *J. Clin. Oncol.* **2010**, *28*, 1780−1787.

(20) Rasi, G.; Terzoli, E.; Izzo, F.; Pierimarchi, P.; Ranuzzi, M.; Sinibaldi-Vallebona, P.; Tuthill, C.; Garaci, E. Combined treatment with thymosin-alpha1 and low dose interferon-alpha after dacarbazine in advanced melanoma. *Melanoma Res.* **2000**, *10*, 189−192.

(21) Shen, X.; Li, Q.; Wang, F.; Bao, J.; Dai, M.; Zheng, H.; Lao, X. Generation of a novel long-acting thymosin alpha1-Fc fusion protein and its efficacy for the inhibition of breast cancer in vivo. *Biomed. Pharmacother.* **2018**, *108*, 610−617.

(22) Lao, X.; Li, B.; Liu, M.; Shen, C.; Yu, T.; Gao, X.; Zheng, H. A modified thymosin alpha 1 inhibits the growth of breast cancer both in vitro and in vivo: suppressment of cell proliferation, inducible cell apoptosis and enhancement of targeted anticancer effects. *Apoptosis* **2015**, *20*, 1307−1320.

(23) Wang, F.; Li, B.; Fu, P.; Li, Q.; Zheng, H.; Lao, X. Immunomodulatory and enhanced antitumor activity of a modified thymosin alpha1 in melanoma and lung cancer. *Int. J. Pharm.* **2018**, *547*, 611−620.

(24) Wang, F.; Xu, C.; Peng, R.; Li, B.; Shen, X.; Zheng, H.; Lao, X. Effect of a C-end rule modification on antitumor activity of thymosin alpha1. *Biochimie* **2018**, *154*, 99−106.

(25) Teesalu, T.; Sugahara, K. N.; Kotamraju, V. R.; Ruoslahti, E. C-end rule peptides mediate neuropilin-1-dependent cell, vascular, and tissue penetration. *Proc. Natl. Acad. Sci. U.S.A.* **2009**, *106*, 16157−16162.

(26) Sugahara, K. N.; Braun, G. B.; de Mendoza, T. H.; Kotamraju, V. R.; French, R. P.; Lowy, A. M.; Teesalu, T.; Ruoslahti, E. Tumor-penetrating iRGD peptide inhibits metastasis. *Mol. Cancer Ther.* **2015**, *14*, 120−128.

(27) Sugahara, K. N.; Scodeller, P.; Braun, G. B.; de Mendoza, T. H.; Yamazaki, C. M.; Kluger, M. D.; Kitayama, J.; Alvarez, E.; Howell, S. B.; Teesalu, T.; Ruoslahti, E.; Lowy, A. M. A tumor-penetrating

peptide enhances circulation-independent targeting of peritoneal carcinomatosis. *J. Controlled Release* **2015**, *212*, 59−69.
(28) Pellinen, T.; Arjonen, A.; Vuoriluoto, K.; Kallio, K.; Fransen, J. A. M.; Ivaska, J. Small GTPase Rab21 regulates cell adhesion and controls endosomal traffic of beta1-integrins. *J. Cell Biol.* **2006**, *173*, 767−780.
(29) Qin, X.; Yan, M.; Zhang, J.; Wang, X.; Shen, Z.; Lv, Z.; Li, Z.; Wei, W.; Chen, W. TGFbeta3-mediated induction of Periostin facilitates head and neck cancer growth and is associated with metastasis. *Sci. Rep.* **2016**, *6*, 20587.
(30) Wu, X.; Jia, J.; You, H. Thymosin alpha-1 treatment in chronic hepatitis B. *Expert Opin. Biol. Ther.* **2015**, *15*, 129−132.
(31) Yang, Y.-F.; Zhao, W.; Zhong, Y.-D.; Yang, Y.-J.; Shen, L.; Zhang, N.; Huang, P. Comparison of the efficacy of thymosin alpha-1 and interferon alpha in the treatment of chronic hepatitis B: a meta-analysis. *Antiviral Res.* **2008**, *77*, 136−141.
(32) Chien, R.-N.; Liaw, Y.-F.; Chen, T.-C.; Yeh, C.-T.; Sheen, I.-S. Efficacy of thymosin alpha1 in patients with chronic hepatitis B: a randomized, controlled trial. *Hepatology* **1998**, *27*, 1383−1387.
(33) Garaci, E.; Mastino, A.; Pica, F.; Favalli, C. Combination treatment using thymosin alpha 1 and interferon after cyclophosphamide is able to cure Lewis lung carcinoma in mice. *Cancer Immunol. Immunother.* **1990**, *32*, 154−160.
(34) Rasi, G.; Silecchia, G.; Sinibaldi-Vallebona, P.; Spaziani, E.; Pierimarchi, P.; Sivilia, M.; Tremiterra, S.; Garaci, E. Anti-tumor effect of combined treatment with thymosin alpha 1 and interleukin-2 after 5-fluorouracil in liver metastases from colorectal cancer in rats. *Int. J. Cancer* **1994**, *57*, 701−705.
(35) Kammertoens, T.; Friese, C.; Arina, A.; Idel, C.; Briesemeister, D.; Rothe, M.; Ivanov, A.; Szymborska, A.; Patone, G.; Kunz, S.; Sommermeyer, D.; Engels, B.; Leisegang, M.; Textor, A.; Fehling, H. J.; Fruttiger, M.; Lohoff, M.; Herrmann, A.; Yu, H.; Weichselbaum, R.; Uckert, W.; Hübner, N.; Gerhardt, H.; Beule, D.; Schreiber, H.; Blankenstein, T. Tumour ischaemia by interferon-gamma resembles physiological blood vessel regression. *Nature* **2017**, *545*, 98−102.
(36) Listopad, J. J.; Kammertoens, T.; Anders, K.; Silkenstedt, B.; Willimsky, G.; Schmidt, K.; Kuehl, A. A.; Loddenkemper, C.; Blankenstein, T. Fas expression by tumor stroma is required for cancer eradication. *Proc. Natl. Acad. Sci. U.S.A.* **2013**, *110*, 2276−2281.
(37) Folkman, J. Tumor angiogenesis: therapeutic implications. *N. Engl. J. Med.* **1971**, *285*, 404−405.
(38) Delisser, H. M.; Baldwin, H. S.; Albelda, S. M. Platelet Endothelial Cell Adhesion Molecule 1 (PECAM-1/CD31): A Multifunctional Vascular Cell Adhesion Molecule. *Trends Cardiovasc. Med.* **1997**, *7*, 203−210.
(39) Zhang, Y.-Y.; Kong, L.-Q.; Zhu, X.-D.; Cai, H.; Wang, C.-H.; Shi, W.-K.; Cao, M.-Q.; Li, X.-L.; Li, K.-S.; Zhang, S.-Z.; Chai, Z.-T.; Ao, J.-Y.; Ye, B.-G.; Sun, H.-C. CD31 regulates metastasis by inducing epithelial-mesenchymal transition in hepatocellular carcinoma via the ITGB1-FAK-Akt signaling pathway. *Cancer Lett.* **2018**, *429*, 29−40.
(40) Lutzky, V. P.; Carnevale, R. P.; Alvarez, M. J.; Maffia, P. C.; Zittermann, S. I.; Podhajcer, O. L.; Issekutz, A. C.; Chuluyan, H. E. Platelet-endothelial cell adhesion molecule-1 (CD31) recycles and induces cell growth inhibition on human tumor cell lines. *J. Cell. Biochem.* **2006**, *98*, 1334−1350.
(41) Pantanowitz, L.; Moses, A. V.; Früh, K. CD31 immunohistochemical staining in Kaposi Sarcoma. *Arch. Pathol. Lab. Med.* **2012**, *136*, 1329. ; author reply 1330
(42) Aguzzi, M. S.; Giampietri, C.; De Marchis, F.; Padula, F.; Gaeta, R.; Ragone, G.; Capogrossi, M. C.; Facchiano, A. RGDS peptide induces caspase 8 and caspase 9 activation in human endothelial cells. *Blood* **2004**, *103*, 4180−4187.
(43) Hu, C.; Jiang, X. Role of NRP-1 in VEGF-VEGFR2-Independent Tumorigenesis. *Target Oncol.* **2016**, *11*, 501−505.
(44) Ruoslahti, E. The RGD story: a personal account. *Matrix Biol.* **2003**, *22*, 459−465.
(45) Teesalu, T.; Sugahara, K. N.; Ruoslahti, E. Tumor-penetrating peptides. *Front. Oncol.* **2013**, *3*, 216.
(46) Jia, T.; Choi, J.; Ciccione, J.; Henry, M.; Mehdi, A.; Martinez, J.; Eymin, B.; Subra, G.; Coll, J.-L. Heteromultivalent targeting of integrin alphavbeta3 and neuropilin 1 promotes cell survival via the activation of the IGF-1/insulin receptors. *Biomaterials* **2018**, *155*, 64−79.

https://dx.doi.org/10.1021/acsomega.0c00220
ACS Omega 2020, 5, 10374−10381